

M agnetic and superconducting properties of $\text{Cd}_2\text{Re}_2\text{O}_7$: Cd N M R and R e N Q R .O .V yaselev,^{1,2} K .A rai,¹ K .K obayashi,¹ J .Y am azaki,¹ K .K odam a,¹ M .T akigawa,¹ M .H anawa,¹ and Z .H iroi¹¹Institute for Solid State Physics, University of Tokyo 5-1-5 Kashiwanoha, Kashiwa, Chiba 277-8581, Japan²Institute of Solid State Physics Rus. A c. Sci., Chemogolovka Mosc. Distr., 142432 Russia

(Dated: M arch 22, 2024)

We report Cd N M R and R e N Q R studies on $\text{Cd}_2\text{Re}_2\text{O}_7$, the first superconductor among pyrochlore oxides ($T_c \sim 1$ K). R e N Q R spectrum at zero magnetic field below 100 K rules out any magnetic or charge order. The spin-lattice relaxation rate below T_c exhibits a pronounced coherence peak and behaves within the weak-coupling BCS theory with nearly isotropic energy gap. Cd N M R results point to moderate ferromagnetic enhancement at high temperatures followed by rapid decrease of the density of states below the structural transition temperature of 200 K.

The pyrochlore transition metal oxides with the chemical formula $\text{A}_2\text{B}_2\text{O}_7$ known for decades have recently attracted renewed interest. A and B sublattices both form a network of corner-sharing tetrahedra. The geometry of such a lattice causes strong frustration of magnetic interaction when occupied by local moments, resulting in large degeneracy of the low energy states and anomalous magnetic behavior [1]. Interplay between strong correlation and geometrical frustration in itinerant electron systems is a challenging issue. For example, large degeneracy due to frustration is considered to be crucial also for the heavy electron behavior of the spinel compound LiV_2O_4 [2], where V sites form the identical pyrochlore lattice. Recent investigations of pyrochlores including 5d transition metal elements have led to the discovery of the superconductivity, for the first time among pyrochlore oxides, in $\text{Cd}_2\text{Re}_2\text{O}_7$ below $T_c \sim 1$ K [3, 4, 5] and unusual metal-insulator transition in $\text{Cd}_2\text{Os}_2\text{O}_7$ [6].

Besides superconductivity, $\text{Cd}_2\text{Re}_2\text{O}_7$ shows an unusual phase transition at 200 K [3, 7, 8]. Although complete structural determination below 200 K is yet to be done, X-ray studies proposed a second-order transition from the high-temperature (high-T) cubic $\text{Fd}\bar{3}m$ space group to the low-T cubic $\text{F}\bar{4}3m$ space group [7], accompanied by loss of inversion symmetry at Re and Cd sites. The transition also causes a large change of electronic properties [3, 8]. The resistivity shows almost no T-dependence near room temperature but drops abruptly below 200 K. The magnetic susceptibility also decreases steeply below 200 K, while at higher temperatures it shows only weak T-dependence with a broad maximum near 300 K. Moreover, a kink in resistivity near 120 K indicates an additional phase transition [7, 9]. Results of band structure calculations [10, 11] indicate that the material is a compensated semiconductor with two electron (one hole) Fermi surfaces centered at the (K) point of the $\text{Re-5d}(t_{2g})$ bands. The electronic structure near the Fermi level is sensitive to structural distortion. While it is proposed that a structural transition may occur to remove large spin degeneracy of localized moments on a pyrochlore lattice [12], relation between structure and electronic properties is largely unexplored for itiner-

ant electron systems.

In this letter we describe the microscopic information on the magnetic and superconducting properties of $\text{Cd}_2\text{Re}_2\text{O}_7$ obtained from the nuclear magnetic resonance (N M R) at Cd sites and the nuclear quadrupole resonance (N Q R) at Re sites. The procedure of growing single crystals of $\text{Cd}_2\text{Re}_2\text{O}_7$ has been described earlier [3]. N M R measurements were done on a single crystal in the external field of 10.47 T. For N Q R, a crystal was crushed into powder. Standard spin-echo pulse techniques were used, including inversion-recovery to measure spin-lattice relaxation rate.

We first discuss the low-temperature N Q R results on Re sites. N Q R spectra of ^{185}Re and ^{187}Re nuclei, both with spin 5/2, have been obtained below 100 K. Measurements at higher temperatures were hampered by short spin-spin relaxation time. The spectra at 5 K are shown in Fig. 1 where the top and the bottom panels correspond to $3/2 \leftrightarrow 1/2$ and $5/2 \leftrightarrow 3/2$ transitions, respectively. N Q R frequency of spin 5/2 nucleus can be expressed as [18]: $\nu_{5/2 \leftrightarrow 3/2} = \frac{3}{2} \nu_Q [1 + (59/54) \eta^2]$ and $\nu_{3/2 \leftrightarrow 1/2} = \frac{1}{2} \nu_Q [1 - (11/54) \eta^2]$, where $\nu_Q / \nu_{zz} =$

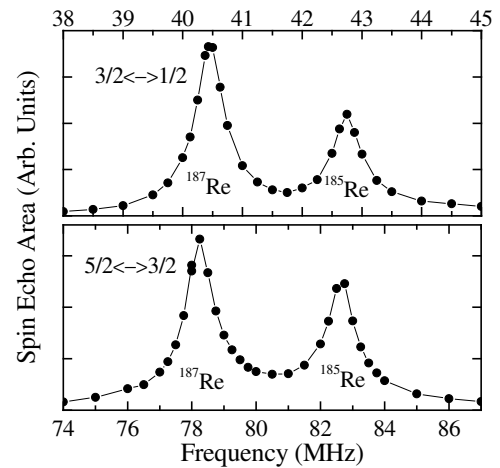


FIG. 1: R e N Q R spectra at 5 K. Top panel: $3/2 \leftrightarrow 1/2$ transition. Bottom panel: $5/2 \leftrightarrow 3/2$ transition.

$\partial^2 V / \partial z^2$ is the largest principal value of the electric field gradient (EFG) tensor at the nuclear position, V is the electrostatic potential, and $\eta = (V_{xx} - V_{yy}) / V_{zz}$ is the asymmetry parameter. Applying these expressions to the measured spectra one finds $Q = 40.4 \text{ MHz}$ at 5 K , gradually decreasing with temperature to 37.6 MHz at 100 K , and $\eta = 0.166 \pm 0.002$ without noticeable temperature dependence.

A sharp line for each NQR transition of both Re isotopes immediately rule out nonuniform charge distribution among Re sites such as charge density wave states. Because of the large quadrupole moments of ^{185}Re and high sensitivity of the EFG to the local charge distribution of 5d electrons, any nonuniform charge distribution should give rise to broadening or splitting of the NQR lines. We can also rule out any magnetic order, since $1/\mu_B$ of spin moment in 5d state typically gives the hyperfield of 100 T . Thus even a tiny moment would have caused the Zeeman splitting of the NQR spectra.

Re sites possess threefold rotation symmetry both in the high- T Fd3m structure or in the F43m structure, the latter being proposed by X-ray for the structure below 200 K [7]. Since EFG is a second rank symmetric tensor, it must be axially symmetric in these cases. Therefore, the nonzero value of η implies further lowering of symmetry at least in the temperature range below 100 K .

Fig. 2 shows the spin-lattice relaxation rate $^{187}\text{T}_1^{-1}$ of ^{187}Re nuclei measured on the $5/2 \rightarrow 3/2$ NQR transition at zero magnetic field as a function of inverse temperature. The relaxation was confirmed to be of magnetic (not quadrupolar) origin at several temperatures by observing that the ratio of T_1^{-1} for the two Re isotopes is equal to the squared ratio of the nuclear magnetic moments.

Above T_c in the region $1 \leq T \leq 5 \text{ K}$, $^{187}\text{T}_1^{-1}$ is practically linear in temperature, $^{187}(\text{T}_1 T)^{-1} = 127 \text{ (Sec K)}^{-1}$. Just below T_c , $^{187}\text{T}_1^{-1}$ increases sharply exhibiting a strong coherence peak [13] with a maximum of about 245 (Sec K)^{-1} at 0.88 K , which is twice as large as just above T_c . Below 0.8 K the relaxation rate decreases following an activated T -dependence.

It is well known that a coherence peak in the T -dependence of T_1^{-1} is easily depressed when magnitude of the superconducting gap varies substantially or the order parameter changes sign over the Fermi surface. Thus the observed well-pronounced coherence peak provides a clear evidence for nearly isotropic s-wave superconducting gap. Nodeless gap in this material have been recently inferred also from specific heat data [14] and SR [15, 16] measurements of the penetration depth. We have fitted the data to the BCS expression, considering distribution of the gap due to possible variation over the Fermi surface [17]. We assumed a uniform distribution of the gap between $-\Delta$ and $+\Delta$ and Δ to be independent of temperature. The T -dependence of Δ is assumed to follow the weak coupling BCS theory. A good

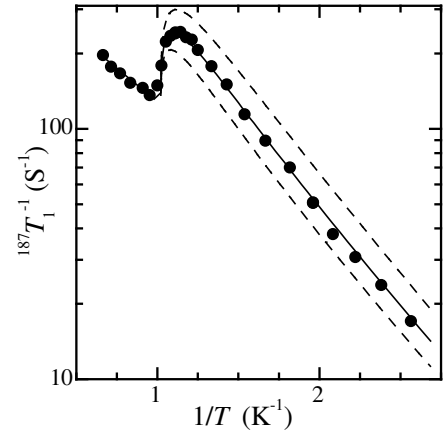


FIG. 2: ^{187}Re spin-lattice relaxation rate vs inverse temperature. The solid line is the fit to the weak coupling BCS theory with $\Delta = 0.22$, $(T = 0) = 1.80 \text{ K}$, and $T_c = 0.98 \text{ K}$. The dashed lines represent the cases with $\Delta = 0.27$ or 0.17 .

fit was obtained for $\Delta = 0.22$, $(T = 0) = 1.80 \text{ K}$, and $T_c = 0.98 \text{ K}$ as shown by the solid line in Fig. 2. The ratio $(T = 0)/T_c = 1.84$ is close to the weak coupling BCS value 1.75 , justifying our analysis. The dashed lines in Fig. 2 indicate that the height of the coherence peak is sensitive to distribution of the gap. The fitted value of Δ puts the upper limit for the gap variation, since any damping of the quasi-particles will also suppress the coherence peak.

Let us now turn to the NMR results on Cd sites. The Knight shift, K , and the spin-lattice relaxation rate, $^{111}\text{T}_1^{-1}$ were measured for ^{111}Cd nuclei (spin $1/2$) using a single crystal. In the high temperature Fd3m structure, threefold rotation symmetry at Cd sites should give rise to the axially symmetric Knight shift, $K = K_{\text{iso}} + K_{\text{ax}}(1 - 3\cos^2\theta)$, where θ is angle between the external field and the $[111]$ direction. This angular dependence was observed above 200 K . Upon cooling below the structural transition temperature (200 K) the line splits in two. The average shift of the split lines follows the same angular dependence and thus the values of the isotropic (K_{iso}) and the axial (K_{ax}) parts of the shift were determined as a function of temperature. Since the splitting is very small (less than 0.018%), the conclusions of the following analysis do not depend on the validity of such averaging.

In Fig. 3a, K_{iso} is plotted against temperature (bottom axis) or magnetic susceptibility, χ (top axis). The axial part K_{ax} (not shown in the figure) is 0.042% at 300 K , much smaller than K_{iso} , and decreases only by 0.01% upon cooling down to 4 K , indicating that the dominant hyperfield comes from the Cd s-states hybridized with the Re 5d conduction states. Similar to the magnetic susceptibility [3], K_{iso} decreases rapidly below 200 K . The shift is generally expressed as $K_{\text{iso}} = K_0 + K_s(T)$, where the first term is the T -

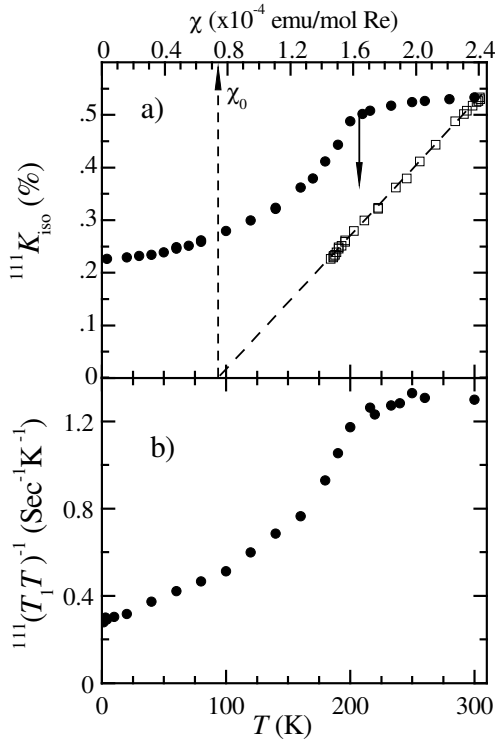


FIG. 3: (a): Isotropic part of ^{111}Cd Knight shift vs temperature (circles { bottom axis), and vs magnetic susceptibility (squares { top axis). (b): Temperature dependence of $(T_1T)^{-1}$ at ^{111}Cd sites.

independent chemical shift and the second term is the T {dependent spin shift from conduction electrons. Likewise $\chi = \chi_0 + \chi_s(T)$, where the first term is the sum of the diamagnetic and the orbital (Van Vleck) susceptibility. As shown in Fig. 3, linear relation was found between K_{iso} and χ in the whole temperature range, yielding the hyperfine coupling constant $A_{\text{hf}} = N_A \mu_B K_s = 17.9 \text{ T} = B$. Since the chemical shift of Cd in a nonmagnetic and nonmetallic substance is typically 0.01 % or less [19] and much smaller than the observed value of K_{iso} , we assume $\text{K}_0 = 0$ in the following analysis. We then obtain $\chi_0 = 0.75 \times 10^{-4} \text{ emu/mole Re}$, leading to $\chi_s = 1.65 \times 10^{-4} \text{ emu/mole Re}$ at 300 K. From the standard value for the diamagnetic susceptibility $\chi_{\text{dia}} = 0.76 \times 10^{-4} \text{ emu/mole Re}$, the orbital susceptibility is estimated as $\chi_{\text{orb}} = 1.51 \times 10^{-4} \text{ emu/mole Re}$.

In Fig. 3b, is shown the T {dependence of $^{111}(T_1T)^{-1}$ measured for Hk[001]. At some temperatures $^{111}\text{T}_1$ was measured for Hk[110] and found to be isotropic. We found that $^{111}(T_1T)^{-1}$ also shows rapid reduction below 200 K, indicating that the phase transition at 200 K causes sudden loss of the density of states (DOS). For noninteracting electrons, when the spin shift and the spin {lattice relaxation are both due to contact interaction with unpaired s {electrons, the Korringa relation is

known to be satisfied, $T_1TK_s^2 = (\mu_e/\mu_n)^2 (\hbar/4k_B) S$, where μ_e and μ_n are respectively electronic and nuclear gyromagnetic ratios. In real metals, the ratio

$$K = S/(T_1TK_s^2) \quad (1)$$

provides a useful measure of magnetic correlation [20, 21]. Since $(T_1T)^{-1}$ probes the dynamical susceptibility averaged over the Brillouin zone, it can be enhanced by either ferromagnetic (FM) or antiferromagnetic (AF) spin correlations, while only FM correlation strongly enhances the spin shift. Thus, generally speaking, the value of K being much smaller (larger) than unity is a signature for substantial FM (AF) correlation.

Solid circles in Fig. 4 show the T {dependence of K . The value of $K \approx 0.28$ above 200 K points to moderate FM enhancement. The sudden increase of K below 200 K can be accounted for by loss of DOS as explained below. However, there is a broad peak in K near 60 K, and at lower temperatures K decreases. Choice of non-zero values for K_0 does not change this behavior, which is already evident in Fig. 3 since $^{111}(T_1T)^{-1}$ keeps decreasing whereas $\text{K}(T)$ becomes nearly flat below 50 K.

In order to examine to what extent the behavior of K is explained by T {dependence of DOS, we utilize a simple RPA expression with a free {electron {like dispersion of the conduction band. This analysis is mainly for qualitative purpose since specific feature of the multiple Fermi surfaces of $\text{Cd}_2\text{Re}_2\text{O}_7$ [10, 11] is not considered. We also neglect possible variation of the matrix elements of the contact interaction over the Fermi surface. Although the good proportionality between K and χ supports such a simple situation, careful examination would be required in future in the light of realistic Fermi surface and wave functions. The Stoner enhancement factor of the spin susceptibility

$$1 = (1 - U\chi_0)^{-1} = \chi_s / \chi_0 = (2 \mu_B / U) \chi_0; \quad \chi_s = U \chi_0; \quad (2)$$

where χ_0 is the DOS at the Fermi level and U denotes the Coulomb repulsion, is related to K by RPA as [20, 21]

$$K_{\text{RPA}} = 2 \int_0^1 \frac{(1-x)^2 dx}{[1 - G(x)]^2}; \quad (3)$$

$G(x) = 0.5 f_1 + (1-x^2) = (2x) g \ln j(1+x) = (1-x) j$. Applying eq. (3) to the experimental data of K , we obtain $1 = (1 - U\chi_0)^{-1} = 7.3$ at 300 K. This value is comparable to the enhancement factor of 4.4 obtained from the calculated DOS value for the room temperature structure (0.58 eV⁻¹ per Re [10]) and the experimental value of χ_s obtained above.

We now determine the T {dependence of DOS or $\chi_s(T)$ from the experimental data of $\chi_s(T)$ by using eq. (2), $\chi_s / \chi_0 = (1 - U\chi_0)^{-1}$, with the initial condition that $1 = (1 - U\chi_0)^{-1} = 7.3$ at $T = 300 \text{ K}$. We then calculate K_{RPA} using eq. (3). The results are shown by the circles in Fig. 4. One can

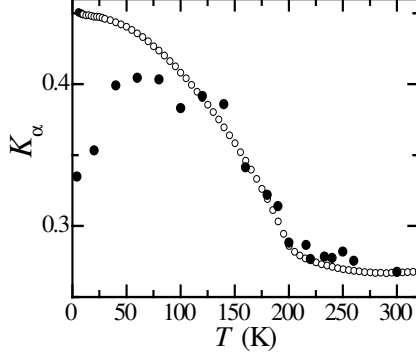


FIG. 4: Temperature dependence of K_α . Filled circles: experimental data of K_α obtained from ^{111}Cd $(T_1T)^{-1}$ and $K_{\text{spin}} = K_{\text{iso}}$ using eqn. (1) Open circles: K_{RPA} calculated from eqs. (2, 3) and the data of χ_s from ref. [3].

see that from high temperatures down to 120 K the calculated K_{RPA} reproduces the experimental data fairly well, supporting our assumption that loss of DOS is the major cause for the reduction of both χ_s and ^{111}Cd $(T_1T)^{-1}$ below 200 K. However, they diverge below 120 K. The anomalous behavior at low temperatures implies that either ferromagnetic enhancement is restored or there is additional suppression only for the dynamical susceptibility.

We found that the ratio of T_1^{-1} at Re and Cd sites is unexpectedly large. Hyperfine interaction between Re nuclei and the 5d conduction electrons should be mainly due to core polarization effect, with typical magnitude $\{120\text{T}/B\}$ [22]. From the values of the hyperfine coupling, the nuclear gyromagnetic ratio and the reduction factor for the relaxation due to core polarization field [23], we expect the ratio $^{187}\text{Tl}^{-1} = ^{111}\text{Tl}^{-1}$ to be 17. Experimentally we obtain $^{187}\text{Tl}^{-1} = ^{111}\text{Tl}^{-1} = 420$ at 5 K. Possible reasons for this may be the following: (1) Orbital hyperfine field gives large contribution to $^{187}\text{Tl}^{-1}$. (2) The hyperfine coupling, in particular for Cd nuclei, is not uniform over the Fermi surface, i.e. some part of the Fermi surface do not couple effectively to Cd nuclei but makes large contribution to the Re relaxation rate. The latter case points to nontrivial magnetic correlation among 5d electrons which does not manifest in the Cd relaxation data.

Finally, we comment on the large reported value of the T-linear coefficient of the specific heat $\gamma = 15 \text{ mJ/K}^2$ above T_c [3]. Our estimate of γ_0 and the susceptibility data in ref. [3] give $\chi_s = 7 \times 10^{-5} \text{ emu/mole Re}$ at 5 K. We then obtain the Wilson ratio $R_W = 0.34$. Such a small value of R_W would normally imply strong electron-phonon coupling and appears to be incompatible with the weak coupling superconductivity. A exotic possibility may be that the large γ is due to low lying excitations which do not contribute to χ_s , for example, orbital uc-

tuations.

In summary, Re NQR data below 100 K reveals no sign of magnetic or charge order in $\text{Cd}_2\text{Re}_2\text{O}_7$. However, asymmetry of electric field gradient indicates lack of threefold rotational symmetry. The superconducting state according to the temperature dependence of Re NQR spin-lattice relaxation rate, is apparently a weak coupling BCS case with a nearly isotropic energy gap. Cd NMR data show moderate ferromagnetic enhancement above 200 K. Rapid decrease of the spin susceptibility and ^{111}Cd $(T_1T)^{-1}$ below the structural phase transition at 200 K is accounted for by loss of the density of states (DOS) down to 120 K. The shift and relaxation rate data at lower temperatures pose puzzles which remain to be clarified.

We would like to thank H. Harima and K. Ueda for enlightening discussion. This work is supported by the Grant-in-Aid for Scientific Research, No. 12400037 and No. 10304027 from the Japan Society for the Promotion of Science (JSPS), and No. 12046219, Priority Area on Novel Quantum Phenomena in Transition Metal Oxides from the Ministry of Education, Culture, Sports, Science and Technology Japan. The research activity of O.V. in Japan is supported by the JSPS Postdoctoral Fellowship for Foreign Researchers in Japan.

-
- [1] A. P. Ramirez et al, Nature 399, 333 (1999).
 - [2] C. Utrano et al, Phys. Rev. Lett. 85, 1052 (2000).
 - [3] M. Hanawa et al, Phys. Rev. Lett. 87, 187001 (2001).
 - [4] H. Sakai et al, J. Phys. Cond. Mat. 13, L785 (2001).
 - [5] R. Jin et al, Phys. Rev. B 64, 180503 (2001).
 - [6] D. Mandrus et al, Phys. Rev. B 63, 195104 (2001).
 - [7] M. Hanawa et al, cond-mat/0109050.
 - [8] R. Jin et al, cond-mat/0108402.
 - [9] Z. Hiroi, private communication.
 - [10] H. Harima, J. Phys. Chem. Solids, to be published.
 - [11] D. J. Singh, P. Blaha, K. Schwarz, and J. O. Sofo, cond-mat/0108226.
 - [12] Y. Yamashita and K. Ueda, Phys. Rev. Lett. 85, 4960 (2000).
 - [13] L. C. Hebel and C. P. Slichter, Phys. Rev. 113, 1504 (1959).
 - [14] Z. Hiroi and M. Hanawa, cond-mat/0111126.
 - [15] M. D. Lumden et al, cond-mat/0111187.
 - [16] R. Kadooni et al, cond-mat/0112448.
 - [17] D. E. M. Laughlin, Solid. State. Physics 31, 1 (1976).
 - [18] A. Abragam, The Principles of Nuclear Magnetism (Oxford University Press, 1961), p. 251.
 - [19] G. C. Carter, L. H. Bennett, and D. J. Kahan, Metallic Shifts in NMR (Pergamon Press, 1977).
 - [20] T. Mori, J. Phys. Soc. Japan 18, 516 (1963).
 - [21] A. Narath, Phys. Rev. 18, 516 (1963).
 - [22] M. Shahan, U. El-Hanany, and D. Zamir, Phys. Rev. B 17, 3513 (1978).
 - [23] Y. Yafet and V. Jaccarino, Phys. Rev. 133, A1630 (1964).